Carbohydrate Research 344 (2009) 113–119

Contents lists available at ScienceDirect

Carbohydrate Research

journal homepage: www.elsevier.com/locate/carres

Chain conformation and rheological behavior of an extracellular heteropolysaccharide Erwinia gum in aqueous solution

Xiaojuan Xu *, Pan Chen, Yin Wang, Lina Zhang

Department of Chemistry, Wuhan University, Wuhan 430072, China

ARTICLE INFO

Article history:
Received 30 June 2008
Received in revised form 5 September 2008
Accepted 7 October 2008
Available online 21 October 2008

Keywords:
Erwinia gum
Polysaccharide
Chain conformation
Rheological behavior

ABSTRACT

The chain conformation of a heteropolysaccharide Erwinia gum (EG) consisting of Glc, Gal, Fuc, and GlcA in aqueous solution was investigated by using viscometry and static and dynamic light scattering. The Huggins constants k' ranging from 0.31 to 0.35, and the larger second virial coefficient A_2 of the order of 10^{-4} and even 10^{-3} mol g^{-2} cm^3 for EG fractions having different molecular weights in 0.03 M NaCl aqueous solution at 25 °C, suggested that 0.03 M NaCl aqueous solution is a good solvent for EG polysaccharide. Smidsrød's '*B*-value' characterizing chain stiffness was estimated to be 0.028–0.045 for EG fractions indicating that the backbone of EG polysaccharide is semi-stiff having similar stiffness to the semi-stiff Alginate and CMC. The hydrodynamic factor ρ (1.69–1.89), Flory-Fox factor Φ, and the product of $\rho\Phi/N_A$ (0.16–0.22) also confirmed the semi-stiffness of EG polysaccharide chains. Compared with general flexible polymers, the first remarkable shear-thinning and then Newtonian flowing behaviors in steady shear tests for EG polysaccharides were ascribed to the alignment of extended semi-stiff chains on shearing. The dynamic oscillatory shear experiments indicated that addition of certain amount of NaCl effectively prohibited its gelation in pure water even at high concentration and low temperature for long time, suggesting that 0.03 M NaCl aqueous solution of EG has good stability and ability of antigelation, and thus is a promising additive in food field.

1. Introduction

In the past one or two decades, solutions of associating polymers, synthetic or naturally occurring, have received much attention of polymer chemists and physicists because of their wide applicability to food additives, cosmetics, paints, and so on.[1,2] Among those polymers, polysaccharides showed more potential because of its unique biodegradability and water solubility. Erwinia (E) gum, produced extracellularly by the strain *Erwinia mituyensis* 5796, is such an industrially useful heteropolysaccharide[3] forming aggregates in aqueous NaCl (0.2 M) even at extremely low polymer concentrations.[4] The major constituting sugars of the original sample are glucose (Glc), galactose (Gal), fucose (Fuc), and glucuronic acid (GlcA) having molar ratios of 3.75:0.72:1.0:1.18 determined by gas chromatography.[3] It is well known that the properties of the polymer materials are basically determined by their chain structure including chemical structure and secondary structure (also chain conformation). Until now, the chemical structure and chain conformation of EG in dilute solution are not yet known. The present study was thus undertaken trying to obtain more information on chemical structure and deduce the global conformation of the polysaccharide molecule in dilute aqueous NaCl.

In general, the global conformation of polymer chains in dilute solution can be deduced from the molecular weight dependence of hydrodynamic properties such as intrinsic viscosity $[\eta]$, diffusion coefficient D, hydrodynamic radius R_h, and statistical thermodynamic properties such as radius of gyration $\langle S^2\rangle^{1/2}$, combined with a worm-like chain model of linear polymers.[5] This requires a broad molecular weight range of homologous components in order to calculate conformation parameters (such as mole mass per contour length M_L, persistence length q, and chain diameter d), because the following have to be taken into account: copolymer effects on the light scattering determination of the weight-average molecular weight M_w, the second virial coefficient A_2, and the z-average radius of gyration $\langle S^2\rangle_z^{1/2}$. For this reason, it is more difficult to evaluate the chain conformation of polymers with heterogeneous components. With new developments in instrumentation of dynamic light or dynamic neutron scattering techniques, dynamic quantities such as the translational diffusion coefficient D, hydrodynamic radius R_h, and the angular dependence of the first cumulant of the dynamic structure factor can be measured with high precision. Another parameter ρ defined as $\langle S^2\rangle^{1/2}/R_h$ could be employed to describe the shape of linear chains to some extent.[6,7] It was found that the estimated ρ parameters of the real long unperturbed polymer chains appear to be correlated to the chain

* Corresponding author. Tel.: +86 27 87219274; fax: +86 27 68754067.
E-mail address: xuxj626@263.net (X. Xu).

0008-6215/$ - see front matter © 2008 Elsevier Ltd. All rights reserved.
doi:10.1016/j.carres.2008.10.009

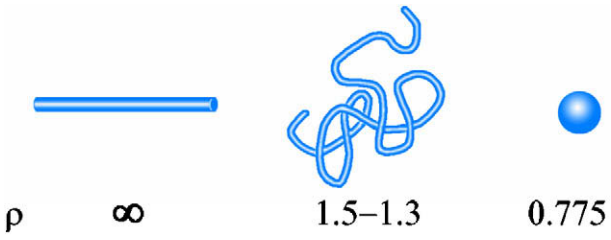

Figure 1. Conformational change from a long rod to a sphere through a random coil with their values of ρ.[7]

stiffness as shown in Figure 1. Therefore, combination of results from static and dynamic light scattering can characterize the chain conformation of polymers.

For a polyelectrolyte, distinctive solution behavior is shown depending on the environmental conditions. Chain conformation evaluation becomes more complicated by using worm-like chain model, because the electrostatic interaction has to be taken into consideration. Furthermore, the electrostatic worm-like chain model was based on several assumptions, resulting in unrealistic parameter estimation. In the early 1970s, Smidsrød and Haug proposed an empirical method, the '*B*-value' method, to evaluate the charge effect for flexible and semi-flexible or semi-stiff polyelectrolytes.[8,9] Their model describes the effect of salt concentration I on $[\eta]$ as follows:

$$[\eta] = [\eta]_{0.1} + S(I^{-0.5} - 0.1^{-0.5}) \quad (1)$$

where $[\eta]_{0.1}$ is the intrinsic viscosity at an ionic concentration equal to 0.1 M. This equation suggests that $[\eta]$ varies approximately as $I^{-0.5}$. They also found that a plot of log$S$ versus log$[\eta]_{0.1}$ for different molecular weight samples was also linear, and deduced the following formula:

$$S = B[\eta]_{0.1}^{\rho} \quad (2)$$

where the power ρ was approximately 1.3 independent on polymer, and B is a proportionality constant which the authors named the '*B*-value', which depends on chain stiffness. This method is very simple and easy to use, and the chain stiffness parameter B can be estimated only from the intrinsic viscosity data. A number of studies showed that Smidsrød's '*B*-value' method is accepted widely, and even applicable to characterize biopolymers such as xanthan,[10] hyaluronate,[11] pectin,[12] alginate,[13] and cellulose derivatives.[14] From these examples, it can be seen that this '*B*-value' method is not only applicable to homopolymers but also to heteropolymers.

In the work reported below, we analyze data of $\langle S^2\rangle_z$, R_h, and $[\eta]$ (the intrinsic viscosity) for EG in aqueous NaCl at 25 °C, and calculate the conformation parameters ρ and B to evaluate the chain stiffness. The rheological behavior in dilute solution was also studied to provide data relevant to its application in food field.

2. Experiment

2.1. Samples

Erwinia gum sample from *Erwinia mituyensis* 5796, which was kindly supplied by Fourth Specialty Chemicals Sales Dept., Asahi Chemical Industry Co., Ltd (Japan), was dispersed in water, and centrifuged to discard the insoluble part and to get the clear solution. The sample in the clear solution was divided into 24 parts by repeating fractional precipitation with the precipitant of 75% ethanol/25% water. Each product was reprecipitated from a water solution in ethanol, washed with ethanol four times, and finally dried in vacuum over a week. From the fractions thus prepared, 4 middle ones were chosen and designated below as EF-1, EF-2, EF-3, and EF-4 in the order of decreasing molecular weight. All the four fractions were dissolved in water again, filtered through glass filters, and lyophilized.

2.2. Fourier transform IR spectra measurements

Fourier transform infrared spectroscopy (FTIR) was recorded on a Nicolet 5700 spectrometer (Nicolet, Minnesota) in a range from 4000 to 400 cm^{-1} using a KBr-pellet method.

2.3. Chain conformation characterization

Inherent viscosity ($\ln\eta_r/c$) and specific viscosities (η_{sp}/c) were measured at 25 °C on conventional Ubbelohde-type capillary viscometer for the EG fractions in water and aqueous solutions with various NaCl concentrations. Solutions were made by mixing the required amounts of the EG fractions and water or aqueous NaCl in a flask stirring gently for a few hours at room temperature. The weight fraction w of the polysaccharide was determined gravimetrically. The mass concentration c (g/cm^3) was calculated from w with the solution density. Each sample solution (6 mL) was loaded into the capillary viscometer and allowed to equilibrate for ~15 min before measuring the efflux time. The flow time was measured to a precision of 0.1 s, and the test solutions were maintained at a constant temperature within ±0.01 °C during the measurements. The kinetic energy correction was always negligible. For polyelectrolyte, Fuoss–Strauss[15] has shown that (η_{sp}/c) versus c plots are strongly concaved upward, and then they proposed an empirical expression to estimate the intrinsic viscosity ($[\eta]$) as follows:

$$\frac{\eta_{sp}}{c} = \frac{[\eta]}{1 + B'c^{1/2}} \quad (3)$$

where c is polymer mass concentration with unit of g/ml and B' is a constant accounting for the interactions of polyelectrolyte. By plotting (c/η_{sp}) versus $c^{1/2}$ a linear relationship can be found with an intercept of $1/[\eta]$ and slope of $B'/[\eta]$. As mentioned in Section 1, EG contains component of GlcA, and behaves like polyelectrolyte in water. Therefore, the $[\eta]$ value in water will be estimated according to Eq. 3. For neutral polymers, the data obtained for η_{sp} and η_r were treated as usual by the following Huggins and Kraemer equations to determine $[\eta]$.

$$\frac{\eta_{sp}}{c} = [\eta] + k'[\eta]^2 c \quad (4)$$

$$\frac{\ln\eta_r}{c} = [\eta] - (0.5 - k')[\eta]^2 c \quad (5)$$

where k' is Huggins coefficient which is a measure of pairwise hydrodynamic interactions between the macromolecules, and is constant for given polymer at given condition. The linear functions were extrapolated to zero concentration to obtain the intrinsic viscosity at the intercept.

Static light scattering (SLS) measurements were carried out to determine weight-average molecular weight M_w and the z-average mean-square radius of gyration $\langle S^2\rangle_z$ for all samples in aqueous NaCl at 25 °C. An ALV/ DLS/SLS-5000E laser goniometer system (ALV/CGS-8F, ALV, Germany) was used for all the measurements with vertically polarized incident light of wavelength 632.8 nm. Pure benzene at 25 °C was used to calibrate the apparatus. The most concentrated solutions of the samples were prepared by continuous stirring at room temperature overnight, and the solutions of lower concentrations were obtained by sequential dilution. The weight concentrations of all test solutions were determined gravimetrically and converted to mass concentrations c by use of

the densities of the solvent. These solutions were optically purified by filtration through Millipore filters of pore size 0.2 μm. The refractive index increment dn/dc was measured at 632.8 nm for EG in 0.03 M aqueous NaCl at 25 °C by use of Optilable DSP differential refractometer and was determined to be 0.14 cm^3/g regardless of the fraction. The excess reduced scattering intensities R_θ obtained as functions of scattering angle θ and polymer mass concentration c were analyzed by use of the Zimm plots of Kc/R_q versus c and Kc/R_q versus q^2. Here, K is the optical constant and k is the magnitude of the scattering vector defined by $q = (4\pi n_0/\lambda_0)\sin(\theta/2)$, with n_0 being the solvent refractive index.

Dynamic light scattering (DLS) has been used to ascertain the size, shape, and dynamics of biological macromolecules and supramolecular assemblies, and to characterize flow and other properties in physiological and biomedical situations.[16] In this work, DLS measurements were carried out to determine the hydrodynamic radius R_h for EG fractions in 0.03 M aqueous NaCl at 25 °C. In all measurements, we used an ALV/DLS/SLS-5000E light scattering goniometer (ALV/CGS-8F, ALV, Germany) with vertically polarized incident light of wavelength 632.8 nm from a He–Ne laser equipped with an ALV/LSE-5003 light scattering electronics and multiple tau digital correlator. Test solutions were prepared and optically purified in the same manner as in the case of SLS measurements. The normalized autocorrelation function $g^{(2)}(t)$ of scattered light intensity was measured at four or five different concentrations and scattering angles ranging from 30° to 90°. The experimental first cumulant Γ[5] at a scattering angle θ for a given solution was evaluated according to the following equation:

$$\ln[g^{(2)}(t) - 1] = -2\Gamma t + \text{const.} \quad (6)$$

where t is the time. In general, Γ contains contributions of various modes of the polymer dynamics at finite q, but only the translational diffusion mode remains at $q \to 0$.[17,18] Thus, the translational diffusion coefficient D_0 at indefinite dilute is estimated from Γ by

$$D_0 = \lim_{\substack{k\to 0 \\ c\to 0}} \Gamma/k^2 \quad (7)$$

The values of Γ are obtained from slopes of the plots of the quantity on the left-hand side of Eq. 6 against t for various values of k and c according to Eq. 6. The hydrodynamic radius R_h is calculated from the Stokes–Einstein relation as follows:

$$R_h = \frac{k_B T}{6\pi\eta_0 D_0} \quad (8)$$

where k_B is the Boltzman constant; T, the absolute temperature; and η_0, the solvent viscosity.

2.4. Rheological measurements

The EG solutions with concentration ranging from 0.2% to 7% were used in the steady shear tests. All steady shear measurements were performed at 25 °C on a Rheometric Scientific ARES strain-controlled rheometer fitted with Couette geometry ($R_1/R_2 = 32/34 = 0.94$) (TA Instruments, New Castle, DE, USA), which was equipped with two transducers having the sensitivity limit of 0.004 and 1 g cm in torque, respectively. The shear rate ranges from 0.02 to 1000 s^{-1}.

Dynamic strain sweep measurements were done at 1 rad/s to determine the linear viscoelastic regime of the EG solution with a strain range from 0.1% to 200%. Dynamic temperature sweeps were performed at 1 rad/s and strain of 20% on the same rheometer mentioned above to determine the values of storage modulus (G') and loss modulus (G'') over the temperature range from 1 to 25 °C. The time dependences of G' and G'' for the EG solutions at fixed frequency of 1 rad/s and 2.6 °C were also investigated. All the dynamic measurements were performed in the linear viscoelastic region.

3. Results and discussion

3.1. FTIR spectra

The FTIR spectra are shown in Figure 2 for three EG fractions: EF-1, EF-2, and EF-3. The IR spectra of the three fractions are almost identical to each other, indicating that they have the same chemical structure, and that they are mainly different in molecular weight. Therefore, the copolymer effects on light scattering experiments can be neglected in the later part. The spectral range 820–900 cm^{-1} is part of a region often referred to as the 'anomeric region' because the vibrational bans for α- and β-configuration are well separated. In the spectra of EG fractions, two absorption peaks at 836 and 919 cm^{-1} were observed and they could be assigned to the C–C stretching vibrations and C–H bending vibrations of α-glucose.[19] The spectral range 1000–1200 cm^{-1} has been suggested to be dominated by contributions from heavy atom, C–C and C–O stretching vibrations, and the absorption bands in spectral range between 1200 and 1500 cm^{-1} are caused mainly by CH deformation vibrations and COH bending vibrations.[20] The spectra show one mode around 1253 cm^{-1} assigned to the C–O stretching mode in the ring. The normal mode at 1424 cm^{-1} was an almost pure CH_2 group vibration. The absorption bands at about 1730 and 1610 cm^{-1} were assigned to C=O of carboxyl symmetrical stretching vibrations[21] and asymmetrical stretching vibrations,[22] respectively. We assigned the bands at 2928 C–H stretching vibration, which is a characteristic absorption peak of sugars. The broad band at 3417 cm^{-1} was assigned to the stretching vibration modes of O–H group and dominated the whole spectra. Based on the analysis of IR spectra, it may be concluded that the sugars mainly exhibit α-configuration and contain carboxyl. We also tried to obtain more detailed structural information by NMR of EG fractions in D_2O, but this gave poorly resolved spectra (not shown) because of high viscosity or gelation of this polysaccharide in D_2O except for the chemical shift of 96.9 ppm for the anomeric carbons with α- configurations and 174 ppm for COOH, confirming the results from IR.

3.2. Dependence of intrinsic viscosity on salt and *B*-value

Figure 3 illustrates the linear plots of (c/η_{sp}) versus $c^{1/2}$ for three EG fractions in water at 25 °C. From the intercept, $[\eta]$ was determined as shown in Table 1. Usually, intrinsic viscosity reflects the hydrodynamic volume of the polymer in solution. The $[\eta]$ value of the EG fractions is significantly higher than that of random coils

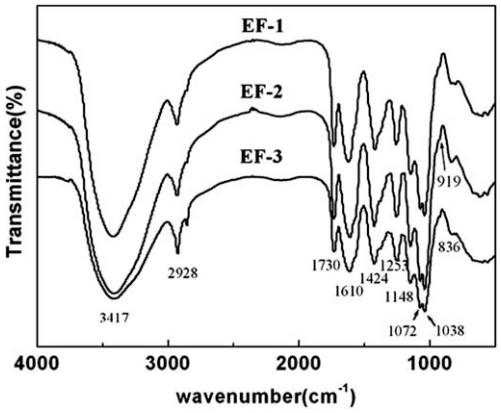

Figure 2. IR spectra of EG fractions EF-1, EF-2 and EF-3 from bottom to top.

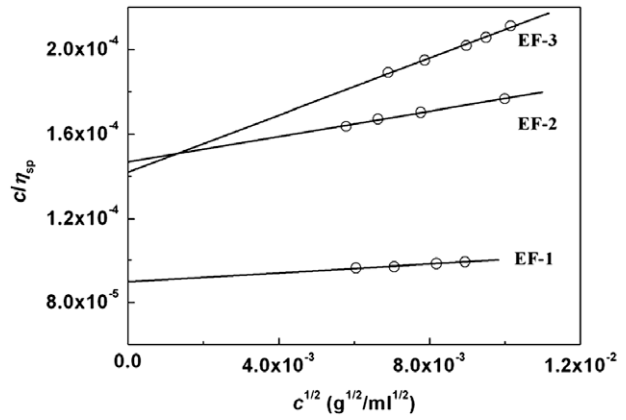

Figure 3. Dependence of c/η_{sp} on $c^{1/2}$ for EG fractions in pure water at 25 °C.

Table 1
Experimental results from viscometry and light scattering for EG fractions in 0.03 M NaCl aqueous solutions and their conformation parameters at 25 °C

Sample	$[\eta]$ (mL/g)		k'	$M_w \times 10^5$ (g/mol)	$\langle S^2\rangle^{1/2}$ (nm)	$A_2 \times 10^4$ (mol cm^3/g^2)	R_h (nm)
EF-1	11,134[a]	2069	0.32	11.1	130.8	8.68	70.2
EF-2	6807[a]	1844	0.32	9.9	125.6	18.87	66.6
EF-3	7040[a]	1358	0.31	7.8	101.5	11.67	59.9
EF-4	—	949	0.35	5.0	82.8	5.90	47.9

[a] In water.

such as well-known polystyrene,[23] amylose,[24] and so forth, revealing that EG exhibits a more extended coil geometry in water at 25 °C.

In NaCl aqueous solutions with NaCl concentrations ranging from 0.01 to 0.2 M, the $[\eta]$ values were estimated according to Huggins and Kraemer equations. Figure 4 shows the plot of Huggins constants k' based on Eqs. 4 and 5 against NaCl concentration for EF-3 in aqueous NaCl. It is well known that the Huggins constant provides an indication of the hydrodynamic interactions of the polymer with the solvent.[25] The Huggins constant usually has values roughly between 0.3 and 0.8 with values of 0.3–0.5 for a polymer in good solvents and 0.5–0.8 for polymers in theta solvents.[26,27] The k' values are 0.3–0.45 for four samples in 0.03 M NaCl aqueous solution, as may be expected for polymers molecularly dispersed in good solvents. Therefore, the later light scattering measurements were performed in 0.03 M NaCl aqueous solution. Moreover, the values of k' increased with increasing salt concentration, which maybe explained by the shielding of the repulsion between the charges located on the macromolecules: as the repulsion increased (lower NaCl concentration) the coil became more extended (less symmetric) and k′ decreased.

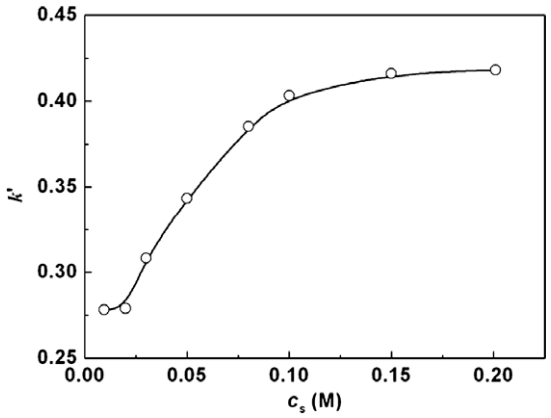

Figure 4. Plot of k' versus salt concentration c_s for EG fraction EF-3 in aqueous NaCl at 25 °C.

Figure 5 shows the salt concentration $I^{-0.5}$ dependence of $[\eta]$ for the four EG fractions. Clearly, $[\eta]$ increased linearly with $I^{-0.5}$, suggesting that this '*B*-value' method could also be applicable to describe the chain conformation of EG. Thus, the *B*-values were calculated from the slopes of the plots according to Eqs. 1 and 2 as shown in Table 2. The *B*-values of EG fractions are significantly higher than those of xanthan, one double helical stiff polysaccharide,[10] but much lower than those of flexible carboxymethylamylose,[14] and close to those of semi-stiff biopolymers, for example, carboxymethylcellulose (CMC) and alginate,[13] indicating that EG also has semi-stiff backbone.

3.3. Data analysis from light scattering

Figure 6 shows the Zimm plot of EF-3 in 0.03 M aqueous NaCl at 25 °C. It is easy to calculate the M_w, $\langle S^2\rangle^{1/2}$ and the second virial coefficient A_2 from this plot. The numerical results of EG fractions are summarized in Table 1 along with those for $[\eta]$. The values of A_2 are on the order of 10^{-4} and even 10^{-3} mol cm^3/g^2 for any fraction, so that the intermolecular interactions between EG chains in the solvent are predominantly repulsive, in accordance with the results from viscometry. The molecular dependence of $\langle S^2\rangle^{1/2}$ and that of $[\eta]$ in the limited molecular weight range (not shown here) were described as $\langle S^2\rangle^{1/2} \sim M_w^{0.58}$ and $[\eta] \sim M_w^{0.97}$, respectively. The former relation with exponent of 0.58 indicates that EG in the M_w range examined behaves like a linear flexible chain expanded by large excluded-volume effect or like a stiff chain with or with-

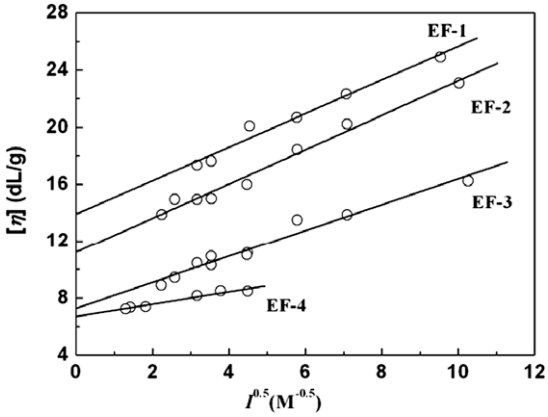

Figure 5. Plots of $[\eta]$ versus $I^{-0.5}$ of EG fractions in aqueous solutions with different ionic strengths at 25 °C.

Table 2
B-values of different polymers with various conformations

Sample	*B*-value	Conformation	Source
EF-1	0.028	Semi-stiff	This work
EF-2	0.036	Semi-stiff	This work
EF-3	0.045	Semi-stiff	This work
EF-4	0.033	Semi-stiff	This work
CMC	0.043	Semi-stiff	Ref. 13
Alginate	0.032	Semi-stiff	Ref. 13
Aeromonas gum	0.076	Semi-flexible	Ref. 36
Carboxymethylamylose	0.2	Flexible	Ref. 14
Xanthan	0.00525	Stiff	Ref. 10

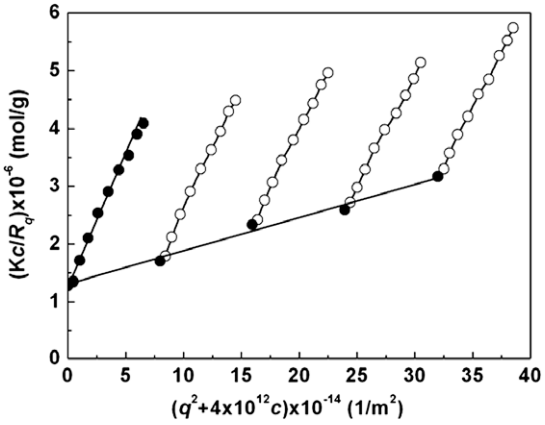

Figure 6. Zimm plot of EG fraction EF-3 in 0.03 M NaCl aqueous solution at 25 °C.

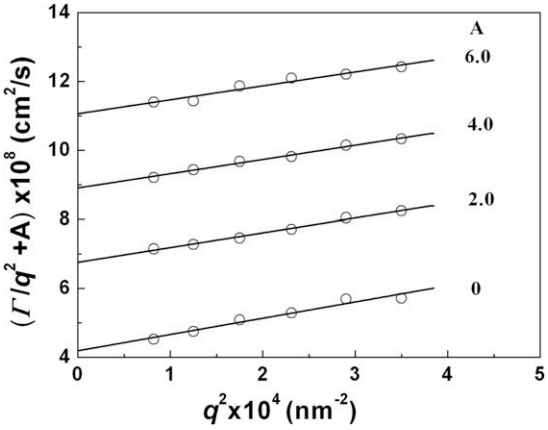

Figure 8. Plots of Γ/q^2 against q^2 for 0.03 M NaCl aqueous solutions of EG fraction EF-3 at 25 °C. The polymer concentrations are 1.99×10^{-4}, 3.99×10^{-4}, 5.99×10^{-4}, 8.00×10^{-4} g/cm^3 from bottom to top. The ordinate values at the respective concentrations are shifted by *A*.

out excluded volume.[28] But the later relation with exponent of 0.97 implies that EG behaves like a semi-stiff chain, similar to the semi-stiff cellulose.[29] Hence, a semi-stiff chain must be a reasonable model for EG.

Figure 7 illustrates $\ln[g^{(2)}(t) - 1]$ data plotted against q^2t at the indicated scattering angles for 0.03 M NaCl aqueous solution of EG fraction EF-3 with a polysaccharide concentration c of 1.9922×10^{-4} g/cm^3. The data points at each angle follow a straight line at first and then a concave curve, which may come from contributions of rotational motions and conformational changes of polysaccharide chains to the dynamical structure factor.[30] From the initial slope of the plot of $\ln[g(2)(t) - 1]$ versus q^2t as shown by dotted lines in Figure 7, the first cumulant Γ divided by q^2 and those at other concentrations for the same fraction EF-3 were estimated according to Eq. 6 and plotted against q^2 in Figure 8. Γ/q^2 shows a weak positive q^2 dependence, but not an anticipated horizontal lines. Other three EG fractions exhibited similar results to those of EF-3. Kubota and Chu[30] also observed nonlinearity in $g^{(2)}(t)$ and positive q^2 dependence of Γ/q^2 for dilute *n*-hexane solutions of semi-stiff poly(*n*-hexyl isocyanate) (PHIC). Fujime and his co-workers analyzed them by the dynamic light scattering theory for worm-like chains, and indicated that conformational changes of semi-flexible polymer chains may affect the q dependence of Γ.[31,32] Therefore, it can be deduced that EG chains might be also semi-stiff, in accordance with results from the empirical '*B*-value' method.

In general, the relation of Γ and q can be described by the scaling formula of $\Gamma \sim q^a$ with the exponent a dependent on $1/q$ and size of the particles. When the particles molecularly disperse in solution, only the translational motion is observed and a is equal to 2; when the polymers form aggregates, the size of the polymer chains is larger than $1/q$ and the internal and rotational motions can be detected with $a = 3$; when the polymer size is comparative to $1/q$, a is 2–3. Figure 9 shows the scattering vector q dependence of the average characteristic line width Γ for EF-3 in 0.03 M NaCl aqueous solution at different concentrations. All the values of exponents (a) indicated in this plot are slightly larger than 2, and show weak concentration dependence. Similar results were observed for other three EG fractions. This may be contributed to the fact that EG is one polyelectrolyte and ionized in aqueous solution resulting in large size of polysaccharide chains especially at lower concentration. Thus, the internal and rotational motions of large particles were also detected in the present case. By extrapolating the plot of Γ/q^2 versus q^2 to zero q^2, the contributions of the rotational motion and conformational change of the polymer chain to the dynamic structure factor can be eliminated. Thus, the $(\Gamma/q^2)_{q=0}$ were obtained from Figure 8, and the concentration dependence of $(\Gamma/q^2)_{q=0}$ for EG fractions was illustrated in Figure 10. It was reported that the concentration dependence of $(\Gamma/q^2)_{q=0}$ is determined by the polymer-chain mobility and thermodynamic force. In good solvents, the former and latter factors are decreasing and increasing functions of c, respectively.[33] The Huggins k' and the

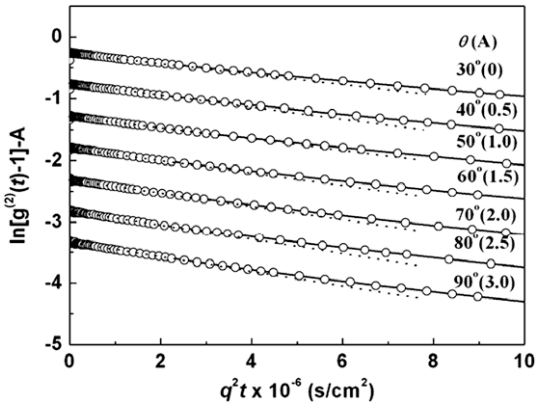

Figure 7. Plots of $\ln[g^{(2)}(t) - 1]$ against q^2t at the indicated scattering angles for a 0.03 M NaCl aqueous solution of EG fraction EF-3 with $c = 1.99 \times 10^{-4}$ g cm^{-3} at 25 °C. The ordinate values at the respective angles are shifted by *A*.

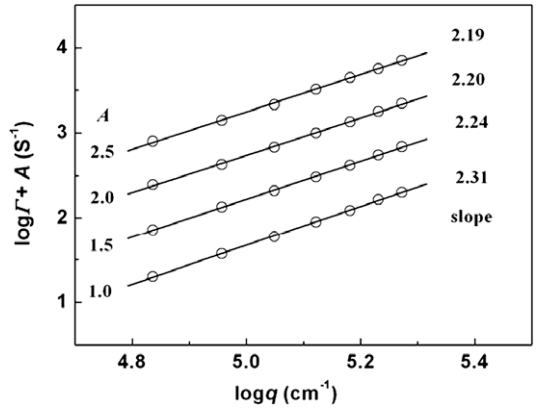

Figure 9. Plots of logΓ against log$q$ for 0.03 M NaCl aqueous solutions of EG fraction EF-3 at 25 °C. The polymer concentrations are 1.99×10^{-4}, 3.99×10^{-4}, 5.99×10^{-4}, 8.00×10^{-4} g/cm^3 from bottom to top. The ordinate values at the respective concentrations are shifted by *A*.

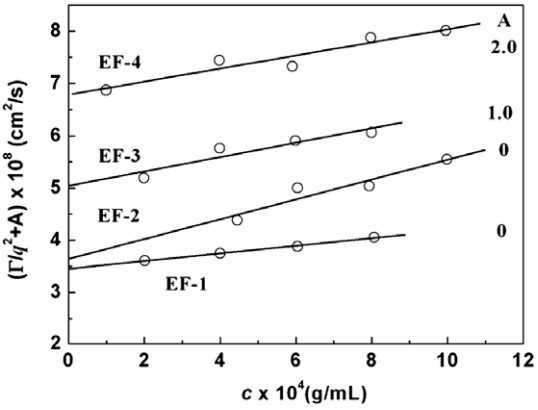

Figure 10. Concentration dependence of $(\Gamma/q^2)_{q=0}$ for the EG fractions in 0.03 M NaCl aqueous solution at 25 °C.

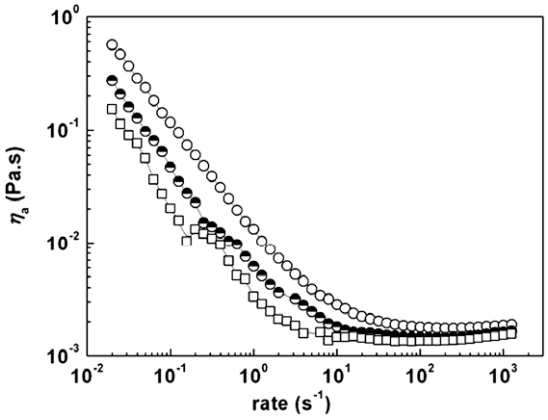

Figure 11. Shear rate dependence of viscosity for EG fraction EF-2 in water at 25 °C. The concentrations are 2.0574×10^{-4}, 2.5535×10^{-4}, and 3.4496×10^{-4} g/cm^3 from bottom to top.

A_2 values have indicated that 0.03 M NaCl aqueous solution is a good solvent of EG. In addition, the mobility decreased with decreasing concentration due to larger size of polysaccharide chains resulted from the ionization of carboxyl for the present case. As a result, a positive concentration dependence of $(\Gamma/q^2)_{q=0}$ was observed. Translational diffusion coefficients D_0 at infinite dilution for the four EG fractions were estimated by extrapolating $(\Gamma/q^2)_{q=0}$ to zero c according to Eq. 7 (cf. Fig. 10). Thus, the hydrodynamic radius R_h for the four EG fractions were calculated according to Eq. 8, and tabulated in Table 1.

3.4. ρ and Φ values

As mentioned in Section 1, the hydrodynamic factor ρ is related with the shape of the polymer chain. By combining the results of $\langle S^2\rangle^{1/2}$ from static light scattering with those of R_h from dynamic light scattering; the ρ values for four EG fractions are calculated and summarized in Table 3. The ρ values ranging from 1.69 to 1.89 are comparable to those for random coils expanded by large excluded-volume effects or for weak stiff chains.[28,34,35] In addition, Flory-Fox factor Φ defined as $[\eta]M_w/(6\langle S^2\rangle)^{3/2}$ were calculated by the data from Table 1 and included together with ρ in Table 3. Obviously, the Φ values are much lower than those of long flexible chains ($\Phi = 1.5–2.8 \times 10^{23}$ mol^{-1}), showing characters of stiff chains.[7] The $\rho\Phi/N_A$ (N_A, Avogadro's number) value is 1.19 for spheres and 0.228 for stiff chains, but lies in the range of 0.3–0.6 for random coils.[7] All the $\rho\Phi/N_A$ values of EG fractions ranging from 0.16 to 0.22 increased very gradually with increasing molecular weight, indicating that EG adopts semi-stiff chain conformation. In a word, all experimental data show that a semi-stiff chain model is applicable to describe the chain conformation of EG. The considerable stiffness of the backbone and the electrostatic repulsion of the COO^- group contributed to the very high viscosity for EG in water as shown in Table 1.

Table 3
ρ and Φ values of EG fractions in 0.03 M NaCl aqueous solution at 25 °C

Sample	ρ ($\equiv\langle S^2\rangle^{1/2}/R_h$)	$\Phi \times 10^{-23}$ (mol^{-1})	$\rho\Phi/N_A$
EF-1	1.86	0.70	0.22
EF-2	1.89	0.62	0.20
EF-3	1.69	0.69	0.19
EF-4	1.73	0.56	0.16

3.5. Rheological behavior

Figure 11 illustrates apparent viscosity data η plotted against shear rate $\dot{\gamma}$ on a double-logarithmic scale for EG fraction EF-2 in 0.03 M NaCl aqueous solution at 25 °C. It is very interesting that the EF-2 aqueous solutions with different concentrations exhibited prominent shear-thinning behavior at first, and then reached the second Newtonian platform in the examined shear rate range of 0.02–1500 s^{-1}. With decreasing concentration, the second Newtonian flowing behavior appeared at lower shear rate. This may be ascribed to the easy alignment of the extended semi-stiff polymer chains. In general, the first Newtonian flowing behavior is observed at low shear rate for flexible polymers even at high concentration, and shear-thinning flowing may occur sometimes. In the present case, remarkable shear-thinning behavior was first observed at very dilute solution for EG fractions, and then the second Newtonian flowing behavior occurred in the examined rate range of 0.02–1500 s^{-1}, implying that EG polysaccharide chains have different conformation from flexible polymer chains. Namely, EG polysaccharide chains possess considerable stiffness, resulting in alignment of the extended stiff chains dominating over the whole system on shearing. Therefore, shear-thinning and second Newtonian flowing behaviors easily occur. This experiment results confirmed the previous conclusions from viscometry and light scattering.

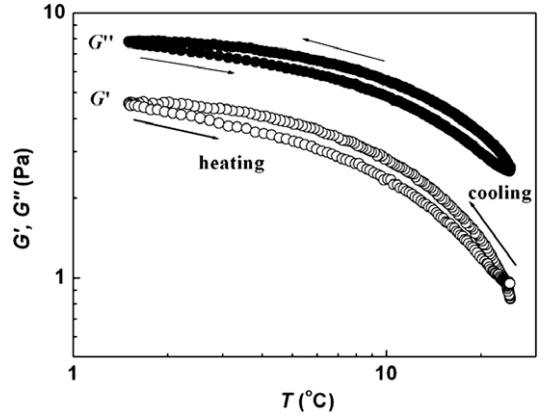

Figure 12. Temperature dependence of G' and G'' of EG fraction EF-2 in 0.03 M NaCl aqueous solution at a concentration of 1.31×10^{-2} g/cm^3 at a frequency of 1 rad/s.

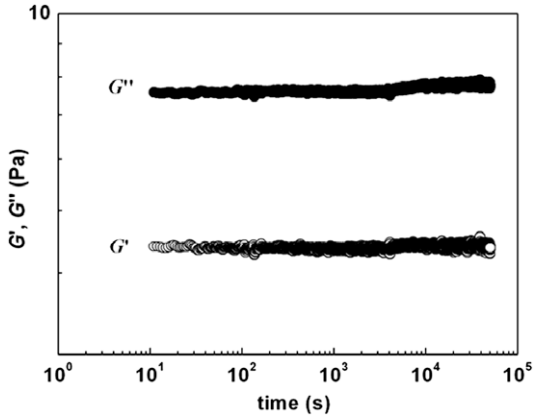

Figure 13. Time dependence of G' and G'' of EG fraction EF-2 in 0.03 M NaCl aqueous solution at a concentration of 1.31×10^{-2} g/cm^3 at a frequency of 1 rad/s, and a strain of 20% at 2.6 °C.

Figure 12 displays the temperature dependence of G' and G'' of EG fraction EF-2 in 0.03 M NaCl aqueous solution at a concentration of 1.31×10^{-2} g/cm^3 at a frequency of 1 rad/s in the cooling and then heating circle. Obviously, G' is much lower than G'' in the examined temperature range of 1–25 °C, suggesting that no gel formation occurred. The data in the cooling process are slightly higher than those in the heating process, implied that there was no obvious structure formation or breaking. The slight hysteresis maybe ascribed to occurrence of aggregation at such high concentration of polysaccharide. Figure 13 demonstrates the time dependence of G' and G'' of EG fraction EF-2 in 0.03 M NaCl aqueous solution at a concentration of 1.31×10^{-2} g/cm^3 at a frequency of 1 rad/s, and a strain of 20% at 2.6 °C. Similarly, G' is much lower than G'' in the whole time range, exhibiting that EG aqueous NaCl solution possesses good solution stability even at low temperature. Namely, addition of NaCl can prohibit gelation of EG in water even at low temperature. All these rheological behaviors show that it is easy to decrease the viscosity of EG by low shear rate, and that the EG solution containing NaCl possesses good stability.

4. Conclusions

The IR spectra showed that EG fractions have similar chemical structure and all the sugars exist as α-configuration. Therefore, the copolymer effects on light scattering experiments can be neglected. The viscomerty and light scattering experiments have shown that EG is molecularly dispersed in 0.03 M NaCl aqueous solution with Huggins constants k' ranging from 0.31 to 0.35 and the larger second virial coefficient A_2 on the order of 10^{-4} and even 10^{-3} mol g^{-2} cm^3. The salt dependence of intrinsic viscosity for EG fractions indicated that EG polysaccharide chains have similar stiffness to the semi-stiff Alginate and CMC by the Smidsrød's '*B*-value' method. The molecular dependence of intrinsic viscosity and radius of gyration also indicated that EG chains adopt semi-stiff chain conformation. The hydrodynamic factor ρ (1.69–1.89), Flory-Fox factor Φ, and their product of $\rho\Phi/N_A$ (0.16–0.22) all confirmed that the semi-stiff-like chain model is applicable to describe the shape of EG polysaccharide chains in 0.03 M NaCl aqueous solutions. The steady rate sweep experiments showed that EG in NaCl aqueous solutions first went through its remarkable shear-thinning behavior but not Newtonian flowing, then reached its second Newtonian platform, also implying that EG chains adopt extended stiff-like chain conformation. The dynamic oscillatory shear experiments indicated that addition of NaCl effectively prohibited its gelation in pure water even at high concentration and low temperature for a long time, suggesting that a 0.03 M NaCl solution of EG has good stability and hence EG has potential in the food industry.

Acknowledgments

This study was funded by the National Natural Science Foundation (20404010 and 20874078), the major grant of the National Natural Science Foundation (30350850) of China, and the High-Technology Research and Development Program of China (2006AA02Z102).

References

1. Dubin, P.; Bock, J.; Davies, R. M.; Schulz, D. N.; Thies, C. Macromolecular Complexes in Chemistry and Biology; Springer: Berlin, 1994.
2. Glass, J. E.. *Associating Polymers in Aqueous Media*. In *ACS Symp. Ser. 765*; Am. Chem. Soc.: Washington, DC, 2001.
3. Tanaka, S. Jpn. Kokai Tokkyo Koho 89 13360, March 6, 1989, 8pp.
4. Zhang, L.; Xu, X.; Pan, S. *J. Polym. Sci.: Part B: Polym. Phys.* **2000**, *38*, 1352–1358.
5. Yamakawa, H. *Helical Wormlike Chains in Polymer Solutions*; Springer: Berlin, 1997.
6. Kajiwara, K.; Burchard, W. *Macromolecules* **1984**, *17*, 2669–2673.
7. Konishi, T.; Yoshizaki, T.; Yamakawa, H. *Macromolecules* **1991**, *24*, 5614–5622.
8. Smidsrød, O. *Carbohydr. Res.* **1970**, *13*, 359–372.
9. Smidsrød, O.; Haug, A. *Biopolymers* **1971**, *10*, 1213–1227.
10. Tinland, B.; Rinaudo, M. *Macromolecules* **1989**, *22*, 1863–1865.
11. Fouissac, E.; Milas, M.; Rinaudo, M.; Borsali, R. *Macromolecules* **1992**, *25*, 5613–5617.
12. Axelos, M. A. V.; Thibault, J.-F. *Int. J. Biol. Macromol.* **1991**, *13*, 77–82.
13. Tobitani, A.; Ross-Murphy, S. B. *Polym. Int.* **1997**, *44*, 338–347.
14. Launay, B.; Doublier, J. L.; Cuvelier, G. In *Functional properties of food macromolecules*; Mitchell, J. R., Ledward, DA., Eds.; Elsevier Applied Science: London, 1986.
15. Fuoss, R. M.; Strauss, U. P. *J. Polym. Sci* **1948**, *3*, 246–263.
16. Pecora, R. *Dynamic Light Scattering*; Plenum Press: New York and London, 1985.
17. Berne, B. J.; Pecora, R. *Dynamic Light Scattering*; John Wiley & Sons: New York, 1976.
18. Doi, M.; Shimada, T.; Okano, K. *J. Chem. Phys.* **1988**, *88*, 4070–4075.
19. Söderholm, S.; Roos, Y. H.; Meinander, N.; Hotokka, M. *J. Raman Spectrosc.* **1999**, *30*, 1009–1018.
20. Gil, E. C.; Colarte, A. I.; El Ghzaoui, A.; Durand, D.; Delarbre, J. L.; Bataille, B. *Eur. J. Pharm. Biopharm.* **2008**, *68*, 319–329.
21. Zhang, H.; Yoshimura, M.; Nishinari, K.; Williams, M. A. K.; Foster, T. J.; Norton, I. T. *Biopolymers* **2001**, *59*, 38–50.
22. Jin, Y.; Zhang, H.; Yin, Y.; Nishinari, K. *Carbohydr. Res.* **2006**, *341*, 90–99.
23. Einaga, Y.; Miyaki, Y.; Fujita, H. *J. Polym. Sci.: Polym. Phys. Ed.* **1979**, *17*, 2103–2109.
24. Nakanishi, Y.; Norisuye, T.; Teramoto, A.; Kitamura, S. *Macromolecules* **1993**, *26*, 4220–4225.
25. Grigorescu, G.; Kulicke, W. M. *Adv. Polym. Sci.* **2000**, *152*, 1–40.
26. Graessley, W. W. *Adv. Polym. Sci.* **1974**, *16*, 1–179.
27. Goh, K. K. T.; Hemar, Y.; Singh, H. *Biopolymers* **2005**, *77*, 98–106.
28. Norisuye, T. *Prog. Polym. Sci.* **1993**, *18*, 543–584.
29. Henley, D. *Ark. Kemi.* **1961**, *18*, 327–392.
30. Kubota, K.; Chu, B. *Macromolecules* **1983**, *16*, 105–110.
31. Fujime, S.; Maruyama, M. *Macromolecules* **1973**, *6*, 237–241.
32. Maeda, T.; Fujime, S. *Macromolecules* **1981**, *14*, 809–818.
33. Ohshima, A.; Yamagata, A.; Sato, T. *Macromolecules* **1999**, *32*, 8645–8654.
34. Fujita, H. *Polymer Solutions*; Elsevier: Amsterdam, 1990.
35. Burchard, W. *Adv. Polym. Sci.* **1999**, *143*, 113–194.
36. Xu, X.; Chen, P.; Zhang, L. *Biorheology* **2007**, *44*, 387–401.